

## INTRANASAL VACCINE BASED ON VIRUS-LIKE PARTICLES FOR COVID-19 PREVENTION: EFFECTS ON BODY WEIGHT, IMMUNOGENICITY AND EFFICACY ASSESSMENT IN HAMSTERS

VALERIA M. KONDRATYEVA<sup>ID</sup>, YANA YU. CHERNORYZH<sup>ID</sup>, VICTOR F. LARICHEV<sup>ID</sup>, IRINA T. FEDYAKINA<sup>ID</sup>,  
OLESYA V. ELISEEVA<sup>ID</sup>, OLEG E. LATYSHEV<sup>ID</sup>, TATYANA V. GREBENNIKOVA\*<sup>ID</sup>

National Research Center for Epidemiology and Microbiology named after honorary academician N. F. Gamaleya, 18 Gamaleya St.-123098, Moscow, Russia

\*Corresponding author: Tatyana V. Grebennikova; \*Email: [t\\_grebennikova@mail.ru](mailto:t_grebennikova@mail.ru)

Received: 29 Aug 2025, Revised and Accepted: 29 Oct 2025

### ABSTRACT

**Objective:** The objective of this study was to comprehensively evaluate the novel intranasal vaccine based on virus-like particles (VLP) in a hamster model, assessing its general toxicity (through clinical observations and body weight dynamics), immunogenicity (by measuring humoral and cellular immune responses), and protective efficacy (by determining the viral load in the lungs after challenge).

**Methods:** 48 female hamsters (*Mesocricetus auratus*) received three intranasal VLP vaccine doses (80 or 120 µg) at 14-day intervals. Toxicity was assessed through clinical observations, weight dynamics, and feed/water consumption. Immunogenicity was evaluated using enzyme-linked immunosorbent assay (ELISA), virus neutralization test (VNT), lymphocyte blast transformation reaction (LBTR), and enzyme-linked immunospot (ELISpot). Viral load in lungs measured efficacy.

**Results:** No behavioral changes, clinical signs, with no mortality. Post-challenge, immunized hamsters (80/120 µg) showed no significant weight loss. Three-dose VLP vaccination induced robust IgG (geometric mean titer: 800 [800–1200] for 80 µg; 1600 [1600–2400] for 120 µg) and neutralizing antibodies (15 [15–20] and 20 [15–30], respectively). It also triggered lymphocyte proliferation (80 µg group,  $p=0.012$ ) and elevated IFN- $\gamma$ -secreting cells (53 and 223 spot-forming units for 80 µg and 120 µg, respectively;  $p<0.001$ ). Vaccine efficacy was demonstrated by significantly lower viral loads in lungs of immunized hamsters ( $2\pm 1.0$  and  $2\pm 1.1$  log tissue culture infectious dose 50% (TCID<sub>50</sub>) for 80 µg and 120 µg) versus controls ( $7\pm 0.8$  log TCID<sub>50</sub>).

**Conclusion:** The VLP-based COVID-19 vaccine demonstrated a favorable safety profile following triple intranasal administration in hamsters, with no adverse effects on body weight and no mortality. The vaccine elicited robust humoral and cellular immune responses, which correlated with strong protection from challenge and significantly reduced viral load in lungs ( $p<0.001$ ), supporting its potential as an effective intranasal vaccine candidate against COVID-19.

**Keywords:** Virus-like particles, VLP vaccine, SARS-CoV-2, COVID-19, Safety, Immunogenicity, Efficacy, Hamsters

© 2026 The Authors. Published by Innovare Academic Sciences Pvt Ltd. This is an open access article under the CC BY license (<https://creativecommons.org/licenses/by/4.0/>) DOI: <https://dx.doi.org/10.22159/ijap.2026v18i1.56676> Journal homepage: <https://innovareacademics.in/journals/index.php/ijap>

### INTRODUCTION

The global spread of SARS-CoV-2, which caused the COVID-19 pandemic, necessitated the urgent development of effective preventive measures. Current research prioritizes the creation of safe, effective, and economically viable vaccines, particularly crucial for resource-limited countries. Key focus areas include developing universal vaccines providing protection against various SARS-CoV-2 strains, as well as formulating thermostable preparations that do not require stringent storage conditions—a critical factor for regions with underdeveloped cold chain infrastructure.

Among emerging platforms, virus-like particles (VLP) uniquely address these requirements by combining high immunogenicity with complete absence of infection risk. By precisely mimicking viral architecture while lacking genetic material, VLP elicits robust humoral and cellular immune responses comparable to natural viral infection. This positions VLP as a complementary platform to mRNA and viral-vector vaccines, particularly for mucosal immunization [1].

To date, over 26 VLP-based vaccine candidates targeting SARS-CoV-2 are in development, with only ~9% (16/183 total candidates in clinical trials) utilizing intranasal delivery (WHO Vaccine Tracker, 2024). Licensed VLP vaccines against human papillomavirus (Gardasil® and Cervarix®) and hepatitis B (Engerix-B® and Recombivax HB®) demonstrate the platform's viability [2].

Despite these advances, no intranasal VLP vaccine has yet achieved clinical approval for COVID-19, highlighting the need for novel approaches. Intranasal VLP vaccines demonstrate unique advantages by inducing immune responses at the primary site of pathogen entry. This approach is pathophysiologically justified, as SARS-CoV-2 cellular

entry occurs via spike (S) protein binding to the angiotensin-converting enzyme 2 (ACE2) receptor, which is highly expressed in the upper respiratory tract epithelium, the main portal of infection. The extrapulmonary manifestations of COVID-19 (lungs, intestines, kidneys) are associated with ubiquitous ACE2 expression, which serves as the primary entry receptor, while the subsequent tissue damage is largely driven by immunopathological mechanisms [3].

Numerous studies demonstrate that intranasal immunization induces both systemic and mucosal immunity, including secretory IgA (sIgA) production in the respiratory tract—the primary site of SARS-CoV-2 replication. This approach confers protection not only against disease progression but also against viral transmission, a critical factor for pandemic control.

Our study addresses key gaps by evaluating a multivalent intranasal VLP vaccine incorporating SARS-CoV-2 structural proteins (S, M, N, E), with S-proteins derived from variants (19A, Alpha, Delta, Omicron). The baculovirus expression system in *Trichoplusia ni* cells enabled high-yield production of properly assembled VLP while preserving conformational epitope integrity [4], while also achieving correct post-translational folding of complex viral glycoproteins, which is essential for preserving conformational epitope integrity.

We selected Syrian hamsters (*Mesocricetus auratus*) as a well-established model for SARS-CoV-2 research, recapitulating key features of human disease: high susceptibility to infection, respiratory viral load dynamics, multiorgan pathology (particularly lung), and age/sex-dependent severity [5].

Crucially, hamsters demonstrate a strong correlation between neutralizing antibody titers and protection levels—making them an

ideal model for preclinical vaccine evaluation. Importantly, findings from this model show excellent translatability to clinical outcomes, as validated during the development of other COVID-19 vaccines.

Therefore, this study aimed to comprehensively evaluate the safety, immunogenicity, and protective efficacy of our multivalent intranasal VLP vaccine against SARS-CoV-2 in this relevant animal model.

## MATERIALS AND METHODS

### Vaccine

The COVID-19 vaccine based on VLP were developed using recombinant technology [6]. The final formulation was an adjuvant-free solution for intranasal administration. The vaccine composition contained a complex of VLP carrying surface S-proteins of SARS-CoV-2 variants (19A, Alpha, Delta, Omicron) produced in a baculovirus expression system (80-120 µg), along with buffer components including potassium dihydrogen phosphate (0.63 mg), disodium hydrogen phosphate (0.65 mg), sodium chloride (3.84 mg), potassium chloride (0.09 mg), calcium chloride (0.02 mg), Tris-HCl (0.03 mg), thimerosal (4.00 µg), and water for injection up to 0.5 ml. Two vaccine formulations with different antigen contents (80 µg and 120 µg per dose) were tested in the study, with 0.9% sodium chloride solution (Grotex, Russia) used as control.

### Animals

The study employed 48 female Syrian hamsters (*Mesocricetus auratus*) aged 6-8 w, obtained from the Stolbovaya Branch of the Scientific Center for Biomedical Technologies (FMBA, Russia). All animals were maintained in vivarium facilities fully compliant with Russian sanitary regulations (SanPiN 3.3686-21), national standards for laboratory animal care (GOST 33215-2014 and GOST 33044-2014), and European guidelines for animal research (Directive 2010/63/EU). The experimental protocol was approved by the Biomedical Ethics Committee of the Gamaleya Research Center

(Protocol #04/2023 dated 07.02.2023), with all procedures, including euthanasia performed according to established ethical standards for animal welfare.

### Cells and viruses

The study utilized the Vero E6 cell line (derived from African green monkey kidney epithelial cells, *Chlorocebus aethiops*), obtained from the Russian National Collection of Cell Cultures at the Gamaleya Research Center (Ministry of Health of Russia). For viral challenge experiments, the SARS-CoV-2 strain PMVL-12 (GISAID accession number EPI\_ISL\_572398) was employed.

### Study design and immunization protocol

6-8 w old 48 hamsters were divided into three equal groups (n=16 per group): Control (0.9% NaCl), VLP-80 (80 µg antigen/dose), and VLP-120 (120 µg antigen/dose). The two antigen doses (80 µg and 120 µg per administration) were selected based on a review of existing literature on VLP-based vaccines and our preliminary studies. The 80 µg antigen/dose was chosen as a dose anticipated to be at the lower threshold of immunogenicity, while the 120 µg antigen/dose represented a higher dose to evaluate a potential increase in immune response. This range was deemed sufficient to assess the vaccine's safety and efficacy profile and to identify a potential dose-response relationship without the need for an excessively broad dose-ranging study at this stage of development. Animals received three intranasal immunizations at 14 d intervals (Days 0, 14, 28) using a pipette dispenser to administer 70 µl total volume (35 µl per nostril) while maintaining supine positioning.

### Immunological assessments

Blood (0.7-0.8 ml) and splenocytes were collected from subgroups (n=4/group/timepoint) at 10-14 days post-each immunization via: gum vein puncture (blood) under anesthesia, splenectomy after euthanasia (ether anesthesia/cervical dislocation) (fig. 1).

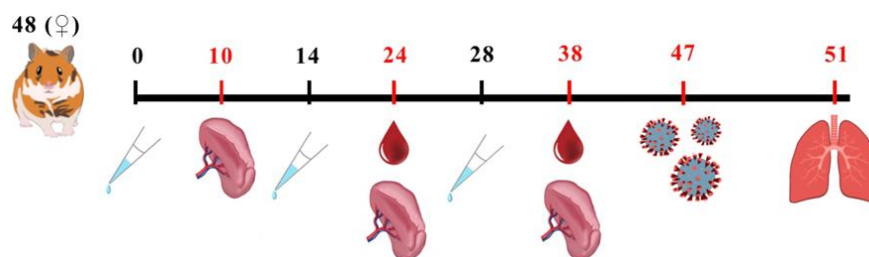


**Fig. 1: Study design.** Female Syrian hamsters aged 6 to 8 w (n = 48) were randomly divided into three groups (n=16 per group): Control (0.9% NaCl), VLP-80 (80 µg/dose), and VLP-120 (120 µg/dose). Animals received three intranasal immunizations (70 µl\*\* total volume) on days 0, 14, and 28 (indicated by syringe symbols). Blood samples (0.7-0.8 ml) were collected from a subgroup of hamsters (n=4 per group per time point) via gum vein puncture under anesthesia 10-14 days after each immunization. Splenocytes were isolated from the same subgroups following euthanasia. On day 47, all remaining animals were intranasally challenged with 10<sup>5</sup> tissue culture infectious dose 50% (TCID<sub>50</sub>) of SARS-CoV-2 (strain PMVL-12). Lungs were collected for viral titer determination on day 51 (4 days post-infection) after terminal anesthesia

### Viral challenge and tissue collection

On day 47 (19 d post-final immunization), all remaining animals were intranasally challenged with 10<sup>5</sup> TCID<sub>50</sub> SARS-CoV-2 (PMVL-12 strain; 50 µl/nostril). Premedication with "Xyla" veterinary anesthetic (Interchemie Werken De Adelaar, Estonia; active ingredient: xylazine hydrochloride) 1 mg/kg prevented sneezing reflexes during procedures. Lungs were collected on day 51 (4 d post-infection) following terminal anesthesia.

### Animal monitoring

Throughout the experiment, daily examinations of hamsters were conducted, assessing their behavior, response to stimuli, and coat condition. On vaccination days, continuous monitoring was performed for one hour following VLP vaccine administration. Body weight measurements were taken using Scout SPX1202 electronic scales (OHAUS, China) starting from day zero of the experiment at 3-day intervals, and then daily after coronavirus infection until the end

of the experiment. Data are presented as group mean values with standard deviations and 95% confidence intervals (m±SD [95% CI]).

### Enzyme-linked immunosorbent assay (ELISA)

The indirect ELISA methodology was performed as previously described [7]. Briefly, recombinant receptor-binding domain (RBD) protein was adsorbed onto microplate wells in 0.1 M carbonate buffer (pH 9.5) at a concentration of 5 µg/ml (100 µl per well) and incubated for 16 h at 4 °C. After four washing cycles, 100 µl of hamster serum samples were added to each well and incubated for 1 h at 37 °C. Following plate washing, 0.1 ml of peroxidase-conjugated anti-hamster IgG secondary antibody (1:500 dilution; Catalog #AS111745, Rabbit anti-Hamster IgG (HandL), HRP conjugated, Agrisera, Sweden) was added and incubated for 1 h at 37 °C. After another washing step, 0.1 ml of TMB substrate solution was added and developed for 15 min at room temperature in the dark. The reaction was stopped with 0.1 ml of 1 M H<sub>2</sub>SO<sub>4</sub>, and absorbance at 450 nm (A<sub>450</sub>) was measured using a Multiscan EX spectrophotometer (Thermo, USA).

### Virus neutralization test (VNT)

The level of neutralizing antibodies (NA) against the SARS-CoV-2 S-protein RBD in hamster sera was determined using a VNT. For the assay, Vero E6 cells obtained from the cell culture collection of the Gamaleya National Research Center for Epidemiology and Microbiology (Russian Ministry of Health) were cultured in 96-well plates (Costar, USA) in Eagle's Minimum Essential Medium (EMEM; PanEco, Russia) supplemented with 10% fetal bovine serum. Hamster sera were serially two-fold diluted from 1:5 to 1:640 in EMEM, and 100  $\mu$ l\*\* of each dilution was mixed with 100  $\mu$ l\*\* of SARS-CoV-2 suspension containing 200 TCID<sub>50</sub>. The mixtures were incubated for 1 h at 37 °C, then were transferred to Vero E6 cell monolayers and incubated for 96 h at 37 °C in a 5% CO<sub>2</sub> atmosphere. The results were assessed by light microscopy (Olympus CKX31SF, Japan). The cytopathic effect (CPE) was evaluated qualitatively for each well by comparing it to virus control wells (100% CPE) and cell control wells (0% CPE). A well was scored as positive for neutralization if the cell monolayer remained completely intact, with no signs of CPE. The following controls were included: uninfected cell control (cells only) and virus control (cells infected with the working virus titer). The NA titer was defined as the reciprocal of the highest serum dilution that completely prevented CPE in 100% of the replicates.

### Lymphocyte blast transformation reaction (LBTR) and IFN- $\gamma$ -secreting cell quantification by enzyme-linked immunospot (ELI spot)

The isolation of splenocytes and LBTR methodology were performed as previously described [8]. Briefly, all procedures were conducted under sterile conditions. Spleens were homogenized, and mononuclear cells were isolated using Ficoll density gradient centrifugation (1.077 g/cm<sup>3</sup>; PanEco, Russia). The isolated cells were cultured in 96-well plates with or without specific and nonspecific stimulants: RPMI1640 medium (PanEco, Russia); SARS-CoV-2 virus (strain PMVL-12; GISAID accession EPI\_ISL\_572398); concanavalin A (12.5  $\mu$ g/ml; PanEco, Russia);  $\beta$ -Propiolactone-inactivated Crimean-Congo hemorrhagic fever virus. Proliferation was assessed after 72 h using an inverted microscope (400 $\times$  magnification). LBTR results were expressed as a stimulation index (PSI), calculated as the ratio of the mean number of lymphoblasts observed in stimulated versus unstimulated wells. An PSI>2 was considered positive. For IFN- $\gamma$  ELISpot, the Hamster IFN-gamma ELI Spot PLUS kit (HRP; MabTech, Sweden) was used per the manufacturer's protocol, with the same stimulants as in LBTR. Spot-forming units (SFU) were counted under a stereomicroscope (MBS-10; LOMO, Russia). Results were reported as the difference in SFU per 10<sup>6</sup> cells between antigen-stimulated wells and negative control wells (medium only).

### Virus titration from lung tissue samples

Lung tissues from SARS-CoV-2 infected hamsters were collected aseptically and homogenized in a mortar with DMEM medium

containing 50  $\mu$ g/ml gentamicin (PanEco, Russia). The homogenate was serially diluted (10<sup>-1</sup> to 10<sup>-8</sup>) in six replicates, inoculated onto Vero E6 cell monolayers in 96-well plates, and incubated for 96 h at 37 °C with 5% CO<sub>2</sub>. Viral presence was assessed by cytopathic effect (CPE). The virus titer was determined as the highest dilution causing CPE, with 50% endpoint titration calculated using the Reed and Muench method [9].

### Statistical analysis

All statistical analyses were conducted in SPSS Statistics version 27 (IBM, USA). Prior to analysis, the assumption of normality was evaluated for all datasets using the Shapiro-Wilk test. Data are summarized descriptively based on their distribution: continuous variables with a normal distribution are reported as mean $\pm$ standard deviation (m $\pm$ SD), while non-normally distributed variables are expressed as median and interquartile range (Me [IQR]). Throughout the results, exact p-values are provided to allow for precise interpretation. When data met assumptions of normality and homogeneity of variance (verified by Levene's test), a one-way analysis of variance (ANOVA) was performed. In cases of significant main effects, post-hoc pairwise comparisons were carried out using Fisher's Least Significant Difference (LSD) test. For normally distributed data with violated homogeneity of variance, the Welch ANOVA was utilized, followed by the Games-Howell post-hoc procedure. If data were not normally distributed, the non-parametric Kruskal-Wallis H-test was employed. Upon finding a statistically significant result, subsequent pairwise comparisons were conducted using Dunn's test, incorporating a Bonferroni adjustment. The non-parametric Mann-Whitney U test was applied for comparing two independent groups when the data were not normally distributed. This test was also used for the comparison of viral titers in lung tissue. A p-value of less than 0.05 was considered indicative of statistical significance for all tests.

## RESULTS

### Assessment of general toxicity

#### Clinical observations

Prior to infection, all animals across groups exhibited normal appearance, behavior, and consumption of food and water. Their fur remained dense, glossy, and smooth. Following SARS-CoV-2 infection, control group hamsters displayed distinct clinical signs, including reduced mobility, hunched posture, and dull/ruffled fur-findings absent in both VLP-80 and VLP-120 vaccinated groups. No mortality occurred in any experimental group throughout the study duration.

#### Body weight evaluation

Longitudinal body weight measurements of hamsters are presented in fig. 2.

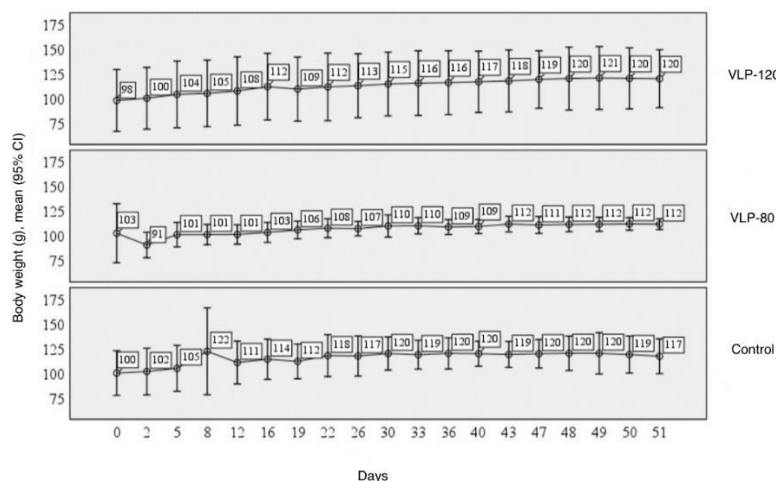


**Fig. 2: Dynamics of body weight in hamsters immunized three times with VLP-based COVID-19 vaccine from day 0 to day 51, with intranasal SARS-CoV-2 infection on day 47. The graph shows body weight (g, left axis) presented as mean values with 95% confidence intervals for each study group: Control, VLP-80, and VLP-120 (indicated at right). The experimental timeline (days) is shown along the bottom axis**

Longitudinal body weight analysis during the vaccination period (days 0-47) revealed no statistically significant differences among the study groups. The data met the assumptions for parametric analysis (homoscedasticity confirmed by Levene's test,  $p > 0.05$ ); thus, a one-way ANOVA with Fisher's F-test was applied. The result was not significant ( $p > 0.05$ ). Consequently, post-hoc pairwise

comparisons were not warranted. mean body weights in all groups showed a non-significant increasing trend from day 0 to day 47, with no substantial weight changes observed in either the control or vaccinated animals, indicating the absence of overt toxicity associated with the vaccine administration. Body weight dynamics before and after the SARS-CoV-2 challenge are detailed in table 1.

**Table 1: Weight changes in study groups following SARS-CoV-2 infection, g**

Groups*	Day post infection					p
	0	1	2	3	4	
Control	119.7±9.0(105.3-134.1)	120.2±10.9 (102.8-137.6)	120.2±13.1 (99.3-141.1)	118.9±11.8 (100.1-137.7)	117.2±11.1 (99.6-134.8)	$p_{1-4}=0.032^{**}$
VLP-80	111.0±5.4 (102.4-119.6)	111.6±4.6 (104.3-118.9)	111.6±4.5 (104.5-118.8)	112.1±4.0 (105.8-118.3)	111.8±3.4 (106.3-117.3)	$p > 0.05$
VLP-120	119.2±18.3 (90.1-148.3)	120.1±20.0 (88.34-151.94)	120.7±20.0 (88.8-152.5)	120.3±19.4 (89.36-151.2)	120.0±18.4 (90.6-149.3)	$p > 0.05$

\*Data are presented as mean±SD with 95% confidence intervals (n=4 per group); \*\*Changes in parameters are statistically significant ( $p < 0.05$ )

Body weight dynamics before and after the SARS-CoV-2 challenge were analyzed using a repeated measures ANOVA. This analysis revealed a significant interaction between the factors 'group' and 'time' ( $p < 0.05$ ). Post-hoc analysis demonstrated a statistically significant reduction in body weight within the control group by day 4 post-infection (from 120.2±10.9 g to 117.2±11.1 g;  $p = 0.032$ ). In contrast, no significant weight changes were observed over time in either the VLP-80 or VLP-120 vaccinated groups ( $p > 0.05$ ). This marked difference in weight dynamics—significant loss in controls versus maintained stability in vaccinated groups—demonstrates that intranasal

VLP vaccination at both tested doses effectively prevented SARS-CoV-2 infection progression.

#### Immunogenicity assessment

##### NA and IgG targeting the SARS-CoV-2 S-protein RBD

The VLP-based vaccine effectively stimulated the production of both RBD-specific IgG and NA following administration at 80 µg and 120 µg antigen doses. As the antibody titer data were non-normally distributed, the results are presented as median with interquartile range (Me [IQR]) in table 2.

**Table 2: Reciprocal titers of NA and anti-RBD IgG in hamsters following the second and third intranasal immunizations with the VLP-based COVID-19 vaccine. Data are expressed as median values with interquartile ranges (Me [IQR]) (n=4 per group)**

Immunisation	Reciprocal titre	VLP 80		VLP 120		p*
		Me	IQR	Me	IQR	
2	IgG	800	600-2000	800	500-2000	0.886
	NA	30	10-40	12.5	2.5-50	0.886
3	IgG	800	800-1200	1600	1600-2400	0.057
	NA	15	10-20	20	15-30	0.486

\*Comparisons between the 80 µg and 120 µg dose groups at each time point were performed using the Mann-Whitney U test.  $p > 0.05$  was considered non-significant.

For comparisons between the two independent dose groups (80 µg vs. 120 µg), statistical analysis was performed using the Mann-Whitney U test. No statistically significant differences in NA or IgG levels were observed between the groups at any time point ( $p > 0.05$ ). Furthermore, comparisons within each group between the 2nd and 3rd immunizations, assessed using the Wilcoxon signed-rank test for paired data, also showed no significant differences ( $p > 0.05$ ). These results indicate that the VLP vaccine is capable of inducing robust specific IgG and NA responses at both tested antigen doses, with no significant boost observed after the third immunization compared to the second.

#### Stimulation index (PSI) and IFN-γ-secreting cell quantification

As demonstrated by Petrov G. *et al.*, triple intranasal immunization with a 120 µg VLP COVID-19 vaccine induced lymphocyte proliferation in hamsters [8]. The current study confirms that the 80 µg dose formulation similarly triggers lymphocyte proliferation following intranasal administration. These results are illustrated in fig. 3.

For comparisons among the three independent experimental groups, the non-parametric Kruskal-Wallis test was used. This analysis revealed that the Stimulation Index (PSI) showed statistically significant differences depending on the experimental group ( $p = 0.032$ ). Post-hoc pairwise comparisons using Dunn's test with Bonferroni correction were subsequently performed. These

comparisons demonstrated that the PSI in the VLP-80 group was significantly higher than in the placebo group ( $p = 0.012$ ), but did not differ from the PSI in the VLP-120 group ( $p = 0.555$ ). The difference between the VLP-120 and placebo groups did not reach statistical significance ( $p = 0.055$ ). Following both the first and second immunizations, animals receiving either the 80 µg or 120 µg antigen dose demonstrated significantly increased lymphocyte proliferation compared to controls, with no dose-dependent differences in PSI values observed. After the third immunization, both vaccinated groups exhibited decreased mean PSI values relative to post-second immunization levels, though these changes were not statistically significant ( $p > 0.05$ ) and remained above threshold values.

#### Antigen-specific IFN-γ response

Stimulation with specific antigen significantly increased the number of IFN-γ-secreting lymphocytes in splenocyte cultures from both VLP-80 and VLP-120 groups (fig. 4).

The cellular immune response was further evaluated by quantifying IFN-γ-secreting cells. For comparison among the experimental groups, ANOVA was conducted. As the data exhibited heteroscedasticity (Levene's test,  $p < 0.05$ ), Welch's F-test was applied. This analysis revealed statistically significant differences in the number of IFN-γ-secreting cells depending on the antigen dose used in the VLP vaccine ( $p < 0.001$ ). Post-hoc analysis using the

Games-Howell test confirmed a dose-dependent increase in IFN- $\gamma$ -secreting cells following the third immunization. Specifically, triple intranasal administration of the VLP vaccine at the 120  $\mu$ g dose

elicited a significantly higher number of IFN- $\gamma$ -producing cells compared to both the control group ( $p = 0.001$ ) and the group immunized with the 80  $\mu$ g dose ( $p = 0.003$ ).

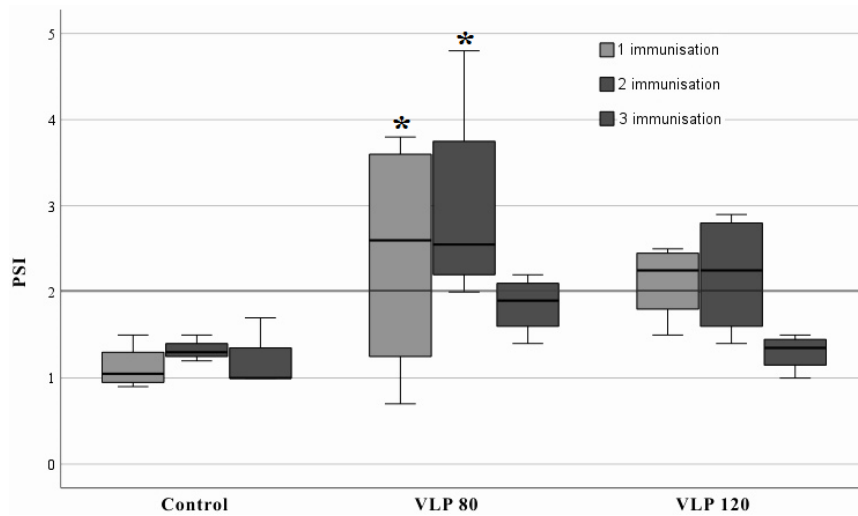


**Fig. 3: Lymphocyte blast transformation response in hamsters 10 d after 1<sup>st</sup>, 2<sup>nd</sup>, and 3<sup>rd</sup> immunizations. Key components: Y-axis: Stimulation index (PSI) of proliferation; X-axis: Experimental groups (Control, VLP-80, VLP-120). Data presentation: mean values with 95% confidence intervals (n=4 per group). \*Changes in parameters are statistically significant ( $p < 0.05$ )**

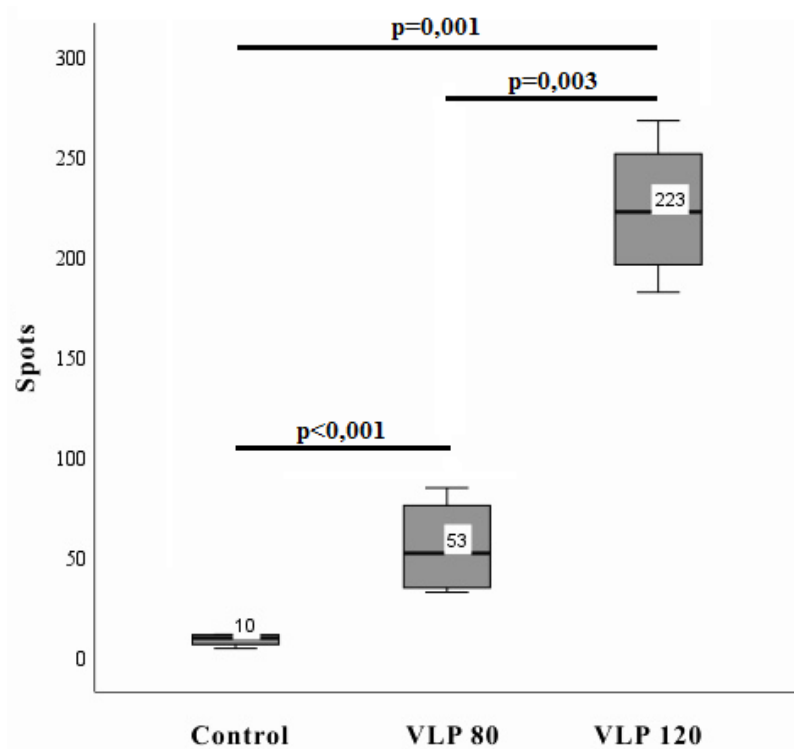


**Fig. 4: Number of IFN- $\gamma$ -secreting cells following antigen-specific stimulation; splenocytes were isolated from hamsters after triple intranasal immunization with VLP-based COVID-19 vaccine. The y-axis shows spot counts (IFN- $\gamma$ -secreting cells per  $10^6$  splenocytes). Data are presented as mean  $\pm$  SD (n=4 per group). The background ELISpot response level for IFN- $\gamma$  was  $\geq 20$ . The x-axis indicates groups: Control, VLP-80, VLP-120**

**Efficacy study**

The evaluation of SARS-CoV-2 infectious titers in the lungs of infected hamsters demonstrated the efficacy of the VLP vaccine. For comparison among the experimental groups, a one-way ANOVA was performed. The data met the assumption of homoscedasticity

(Levene's test for equality of variances,  $p > 0.05$ ); therefore, Fisher's F-test was applied. The analysis revealed statistically significant differences in lung viral titers depending on the antigen dose used for immunization ( $p < 0.001$ ). Post-hoc analysis using Tukey's Honestly Significant Difference (HSD) test was conducted. It confirmed a statistically significant reduction in viral lung titers in

animals receiving triple intranasal immunization with the COVID-19 VLP vaccine compared to the control group, for both the 80 µg dose ( $p < 0.001$ ) and the 120 µg dose ( $p < 0.001$ ). The vaccine reduced viral lung titers from  $7 \pm 0.8 \log \text{TCID}_{50}$  in the control group to  $2 \pm 1.0$  and  $2 \pm 1.1 \log \text{TCID}_{50}$  for the 80 µg and 120 µg doses, respectively. Titers were calculated using the Reed and Muench method.

## DISCUSSION

In the context of ongoing SARS-CoV-2 circulation and the emergence of new viral variants, the development of intranasal vaccines becomes particularly important for preventing both disease and viral transmission. According to the review by Gosavi and Shinde, various vaccine platforms were developed during the pandemic, including inactivated, viral vector, mRNA, and protein subunit vaccines, many of which received emergency use authorization [10]. While this rapid authorization was a necessary measure to control the pandemic, subsequent monitoring revealed serious adverse events, such as Guillain-Barré syndrome. Therefore, the development of immunogenic and, crucially, safe vaccines remains an urgent priority [11, 12]. VLP-based vaccines are of special interest due to their high immunogenicity and safety, as demonstrated in several studies [13-17]. This is further supported by successful applications of similar platforms for other infections such as HPV (Gardasil®, Cervarix®) and hepatitis B (Engerix-B®). Our results are consistent with other studies demonstrating the efficacy of VLP vaccines against SARS-CoV-2. For instance, Lee *et al.*, 2023, showed that an intranasal VLP vaccine with BECC470 adjuvant provided protection against the Delta variant in K18-hACE2 transgenic mice [18], correlating with our data on lung viral load reduction ( $p < 0.001$ , 5 log reduction in viral load). However, unlike their formulation, our vaccine does not require adjuvants to induce a strong immune response, likely due to the optimal structure of multivalent VLP incorporating N, M, E proteins and S-proteins from multiple viral variants.

Resch *et al.*, 2022, demonstrated high immunogenicity of mono- and bivalent VLP vaccines in mice and hamsters, but their intramuscular administration failed to induce local mucosal immunity [19]. In our study, high IgG titers, NA, increased lymphocyte proliferation, and IFN- $\gamma$ -secreting cells confirm the induction of both humoral and cellular immunity. This aligns with known mechanisms of VLP action, where repetitive structures effectively activate B- and T-cell responses. Notably, unlike many modern vaccine candidates, our formulation achieves comparable effects without adjuvants, likely due to optimal VLP size/structure and antigen multivalency. Furthermore, our results demonstrate the advantage of intranasal delivery through the absence of weight loss in vaccinated animals post-challenge, consistent with findings by Lemmer *et al.*, 2024, using plant-based VLP vaccines in hamsters [20].

From a pharmaceutical perspective, comparable efficacy at both tested doses (80 and 120 µg) suggests the potential for optimizing production using lower antigen doses without compromising effectiveness. The comparable humoral immunogenicity and protective efficacy observed with both the 80 µg and 120 µg doses is a notable finding. The absence of a strict dose-response relationship for systemic antibodies could be attributed to the primacy of the mucosal route. Intranasal administration may lead to efficient antigen capture and presentation at the mucosal inductive sites, generating a potent immune response that saturates at a relatively low antigen dose. This contrasts with some parenteral vaccines that often require higher doses or adjuvants to achieve similar efficacy. Therefore, the comparable performance of both doses is not a limitation but rather an indicator of the high efficiency of our intranasal VLP platform. Notably, in our preliminary comparative studies, the immunogenicity and protective efficacy of this VLP formulation were comparable with or without the inclusion of experimental mucosal adjuvants, underscoring the intrinsic potency of the assembled particles. The adjuvant-free formulation simplifies manufacturing and enhances product stability, particularly valuable for resource-limited settings. Additionally, intranasal administration may improve vaccination compliance, especially in pediatric populations and needle-averse individuals—a significant advantage given that most current vaccine candidates require adjuvant systems for similar immune responses.

However, the transition to clinical trials requires further investigation of immune response duration and efficacy against circulating variants. The platform's potential adaptation for combined vaccines against multiple respiratory pathogens represents an interesting future direction. While limitations related to animal models don't diminish the results' significance, they highlight important research avenues, particularly regarding sIgA dynamics and other mucosal immunity markers not assessed in this study. A key limitation of the present work is the absence of secretory sIgA measurement in the respiratory tract mucosa, which is a paramount mechanism of action for intranasal vaccines and a critical endpoint for future evaluation. It should be noted that the developed vaccine, the preclinical studies of which are presented in this paper, is currently undergoing Phase III clinical trials (protocol VLP-IN-III/IV-06/24, approved by the Russian Ministry of Health). Phases I/II, and III clinical trials demonstrated sIgA induction, the results of which will be published in subsequent studies.

In conclusion, our results strongly support the promise of this VLP vaccine candidate. Its combination of safety, efficacy, and practicality makes it an excellent candidate for further clinical development, especially considering the growing need for intranasal SARS-CoV-2 vaccines.

## CONCLUSION

The developed intranasal VLP-based COVID-19 vaccine demonstrated a favorable safety profile following triple administration in hamsters, with no adverse effects on body weight and no mortality. The vaccine induced both humoral and cellular immune responses, accompanied by a statistically significant reduction in lung viral load to  $2 \log \text{TCID}_{50}$  ( $p < 0.001$ ) compared to controls.

These findings support the potential of this VLP vaccine as a promising candidate for COVID-19 prevention, meeting modern requirements for safe and effective pharmaceutical products. The platform holds particular promise for developing vaccines against other respiratory infections.

## FUNDING

This work was supported by the Russian Ministry of Health State Research Program "Development of a VLP-based vaccine prototype for COVID-19 prevention" (Registration No. 121032600024-1).

## AUTHORS CONTRIBUTIONS

All authors confirm their compliance with ICMJE authorship criteria. The contributions were distributed as follows: V. M. Kondratyeva – experiment execution, data analysis and interpretation, manuscript preparation; Ya. Yu. Chernoryzh – experiment execution, analysis and statistical processing of the obtained results, manuscript preparation; V. F. Larichev – experiment execution, manuscript preparation; I. T. Fedyakina – experiment execution, manuscript preparation; O. V. Eliseeva – study concept and design; O. E. Latyshev – experiment execution; T. V. Grebennikova – study concept and design, data analysis and interpretation, manuscript preparation, final approval of the version to be published.

## CONFLICT OF INTERESTS

The authors declare no conflict of interest

## REFERENCES

1. Kheirvari M, Liu H, Tumban E. Virus-like particle vaccines and platforms for vaccine development. *Viruses*. 2023 May;15(5):1109. doi: [10.3390/v15051109](https://doi.org/10.3390/v15051109), PMID [37243195](https://pubmed.ncbi.nlm.nih.gov/37243195/), PMCID [PMC10223759](https://pubmed.ncbi.nlm.nih.gov/PMC10223759/).
2. Roldao A, Mellado MC, Castilho LR, Carrondo MJ, Alves PM. Virus-like particles in vaccine development. *Expert Rev Vaccin*. 2010 Oct;9(10):1149-76. doi: [10.1586/erv.10.115](https://doi.org/10.1586/erv.10.115), PMID [20923267](https://pubmed.ncbi.nlm.nih.gov/20923267/).
3. Wu J, Deng W, Li S, Yang X. Advances in research on ACE2 as a receptor for 2019-nCoV. *Cell Mol Life Sci*. 2021 Jan;78(2):531-44. doi: [10.1007/s00018-020-03611-x](https://doi.org/10.1007/s00018-020-03611-x), PMID [32780149](https://pubmed.ncbi.nlm.nih.gov/32780149/), PMCID [PMC7417784](https://pubmed.ncbi.nlm.nih.gov/PMC7417784/).

4. Krammer F, Schinko T, Palmberger D, Tauer C, Messner P, Grabherr R. Trichoplusia ni cells (High Five) are highly efficient for the production of influenza A virus-like particles: a comparison of two insect cell lines as production platforms for influenza vaccines. *Mol Biotechnol*. 2010 Jun;45(3):226-34. doi: [10.1007/s12033-010-9268-3](https://doi.org/10.1007/s12033-010-9268-3), PMID [20300881](https://pubmed.ncbi.nlm.nih.gov/20300881/), PMCID [PMC4388404](https://pubmed.ncbi.nlm.nih.gov/PMC4388404/).
5. Munoz Fontela C, Dowling WE, Funnell SG, Gsell PS, Riveros Balta AX, Albrecht RA. Animal models for COVID-19. *Nature*. 2020 Oct;586(7830):509-15. doi: [10.1038/s41586-020-2787-6](https://doi.org/10.1038/s41586-020-2787-6), PMID [32967005](https://pubmed.ncbi.nlm.nih.gov/32967005/), PMCID [PMC8136862](https://pubmed.ncbi.nlm.nih.gov/PMC8136862/).
6. Latyshev OE, Zaykova ON, Eliseeva OV, Savochkina TE, Chernoryzh YY, Syroeshkin AV. Development production and characterization of SARS-CoV-2 virus-like particles (Coronaviridae: Orthocoronavirinae: Betacoronavirus: sarbecovirus). *Vopr Virusol*. 2024 May;69(2):175-86. doi: [10.36233/0507-4088-226](https://doi.org/10.36233/0507-4088-226), PMID [38843023](https://pubmed.ncbi.nlm.nih.gov/38843023/).
7. Mardanly SG, Avdonina AS, Mamedova SG. Разработка иммуноферментной тест-системы для выявления антител класса IgG к возбудителю COVID-19 в сыворотке (плазме) крови человека [Development of an enzyme-linked immunosorbent assay for the detection of IgG-antibodies to the causative agent of COVID-19 in human serum (plasma)]. *Klin Lab Diagn*. 2020 Dec;65(11):683-7. doi: [10.18821/0869-2084-2020-65-11-683-687](https://doi.org/10.18821/0869-2084-2020-65-11-683-687), PMID [33301657](https://pubmed.ncbi.nlm.nih.gov/33301657/).
8. Petrov GV, Galkina DA, Koldina AM, Grebennikova TV, Eliseeva OV, Chernoryzh YY. Controlling the quality of nanodrugs according to their new property-radiothermal emission. *Pharmaceutics*. 2024 Jan;16(2):180. doi: [10.3390/pharmaceutics16020180](https://doi.org/10.3390/pharmaceutics16020180), PMID [38399241](https://pubmed.ncbi.nlm.nih.gov/38399241/), PMCID [PMC10891502](https://pubmed.ncbi.nlm.nih.gov/PMC10891502/).
9. Reed LJ, Muench H. A simple method of estimating fifty percent endpoints. *Am J Hyg*. 1938;27(3):493-7.
10. Gosavi DD, N Shinde C. COVID-19 vaccines: targets pre-clinical studies mechanisms of action ADRS and rollout in India a journey so far. *Asian J Pharm Clin Res*. 2022;15(12):24-30. doi: [10.22159/ajpcr.2022.v15i12.46003](https://doi.org/10.22159/ajpcr.2022.v15i12.46003).
11. Shanmugam S, James SG, Sriram DK, George M, Guillain Barre syndrome and COVID-19 vaccination: a disconcerting association. *Asian J Pharm Clin Res*. 2022 Oct;15(10):1-3. doi: [10.22159/ajpcr.2022.v15i10.45364](https://doi.org/10.22159/ajpcr.2022.v15i10.45364).
12. Savarinigal JP, Shilpa K, Noufira P, Gafoor A. Guillain barre syndrome following ChAdOx1 nCoV-19 COVID-19 vaccination at an ADR monitoring center in a Tertiary Care Hospital, Kozhikode: a case series. *Asian J Pharm Clin Res*. 2022 Jul;15(7):3-5. doi: [10.22159/ajpcr.2022.v15i7.44821](https://doi.org/10.22159/ajpcr.2022.v15i7.44821).
13. Vakhrusheva AV, Kudriavtsev AV, Kryuchkov NA, Deev RV, Frolova ME, Blagodatskikh KA. SARS-CoV-2 subunit virus-like vaccine demonstrates high safety profile and protective efficacy: preclinical study. *Vaccines (Basel)*. 2022 Aug;10(8):1290. doi: [10.3390/vaccines10081290](https://doi.org/10.3390/vaccines10081290), PMID [36016181](https://pubmed.ncbi.nlm.nih.gov/36016181/), PMCID [PMC9412395](https://pubmed.ncbi.nlm.nih.gov/PMC9412395/).
14. Kostina LV, Filatov IE, Eliseeva OV, Latyshev OE, Chernoryzh YY, Yurlov KI. Study of the safety and immunogenicity of VLP-based vaccine for the prevention of rotavirus infection in neonatal minipig model. *Vopr Virusol*. 2023 Nov;68(5):415-27. doi: [10.36233/0507-4088-194](https://doi.org/10.36233/0507-4088-194), PMID [38156575](https://pubmed.ncbi.nlm.nih.gov/38156575/).
15. Chernoryzh YY, Kondratyeva VM, Malkova AP, Savochkina TE, Eliseeva OV, Latyshev OE. Pre-clinical safety studies of intranasal virus-like particles based vaccine for prevention of COVID-19. *Vopr Virusol*. 2025 Mar;70(1):35-46. doi: [10.36233/0507-4088-278](https://doi.org/10.36233/0507-4088-278), PMID [40233335](https://pubmed.ncbi.nlm.nih.gov/40233335/).
16. Wang Z, Zhou C, Gao F, Zhu Q, Jiang Y, Ma X. Preclinical evaluation of recombinant HFMD vaccine based on enterovirus 71 (EV71) virus-like particles (VLP): immunogenicity efficacy and toxicology. *Vaccine*. 2021 Jul;39(31):4296-305. doi: [10.1016/j.vaccine.2021.06.031](https://doi.org/10.1016/j.vaccine.2021.06.031), PMID [34167837](https://pubmed.ncbi.nlm.nih.gov/34167837/).
17. Salmons B, Lim PY, Djurup R, Cardoso J. Non-clinical safety assessment of repeated intramuscular administration of an EV-A71 VLP vaccine in rabbits. *Vaccine*. 2018 Oct;36(45):6623-30. doi: [10.1016/j.vaccine.2018.09.062](https://doi.org/10.1016/j.vaccine.2018.09.062), PMID [30293762](https://pubmed.ncbi.nlm.nih.gov/30293762/).
18. Lee KS, Rader NA, Miller Stump OA, Cooper M, Wong TY, Shahrer Amin M. Intranasal VLP-RBD vaccine adjuvanted with BECC470 confers immunity against Delta SARS-CoV-2 challenge in K18-hACE2-mice. *Vaccine*. 2023 Jul;41(34):5003-17. doi: [10.1016/j.vaccine.2023.06.080](https://doi.org/10.1016/j.vaccine.2023.06.080), PMID [37407405](https://pubmed.ncbi.nlm.nih.gov/37407405/), PMCID [PMC10300285](https://pubmed.ncbi.nlm.nih.gov/PMC10300285/).
19. Resch MD, Wen K, Mazboudi R, Mulhall Maasz H, Persaud M, Garvey K. Immunogenicity and efficacy of monovalent and bivalent formulations of a virus-like particle vaccine against SARS-CoV-2. *Vaccines (Basel)*. 2022 Nov;10(12):1997. doi: [10.3390/vaccines10121997](https://doi.org/10.3390/vaccines10121997), PMID [36560407](https://pubmed.ncbi.nlm.nih.gov/36560407/), PMCID [PMC9782034](https://pubmed.ncbi.nlm.nih.gov/PMC9782034/).
20. Lemmer Y, Chapman R, Abolnik C, Smith T, Schafer G, Hermanus T. Protective efficacy of a plant-produced beta variant rSARS-CoV-2 VLP vaccine in golden Syrian hamsters. *Vaccine*. 2024 Feb;42(4):738-44. doi: [10.1016/j.vaccine.2024.01.036](https://doi.org/10.1016/j.vaccine.2024.01.036), PMID [38238112](https://pubmed.ncbi.nlm.nih.gov/38238112/).